Positioning in Non-Terrestrial Networks

SOHA EMARA
MASTER´S THESIS
DEPARTMENT OF ELECTRICAL AND INFORMATION TECHNOLOGY
FACULTY OF ENGINEERING | LTH | LUND UNIVERSITY

SONY

Master's Thesis

Positioning in Non-Terrestrial Networks

By

Soha Emara

Department of Electrical and Information Technology (EIT)
Faculty of Engineering, LTH, Lund University
SE-221 00 Lund, Sweden

Supervisors: Buon Kiong Lau (EIT), Zhinong Ying,
Basuki Priyanto (Sony)

Examiner: Fredrik Rusek (EIT)

28 June 2021

Abstract

In 5G communications, Non-terrestrial Network (NTN) is envisioned to complement Terrestrial Network (TN) to increase network availability, scalability and continuity. Positioning of User Equipment (UE) is critical for the operation of NTN. Currently, NTN uses Global Navigation Satellite System (GNSS) for positioning. However, the use of GNSS to complement NTN operation has some drawbacks such as higher cost and high-power consumption.

The aim of this thesis work is to find an alternative solution to NTN positioning by evaluating a candidate positioning signal for NTN and to analyze the impact of different parameters on positioning accuracy. To this end, Positioning Reference Signal (PRS) in 5G NR is investigated for NTN positioning using different configurations. In addition, the impact of different satellite parameters and deployment scenarios on positioning accuracy has been analyzed in simulation. The effect of uncertainty in the satellites' positions has also been investigated. The simulator is implemented on MATLAB and it is based on 5G NR positioning in Third Generation Partnership Project (3GPP) Release 16.

The results show that good positioning accuracy of within a few meters can be reached using downlink time-difference-of-arrival (DL-TDOA) estimates in NTN. Increasing the bandwidth of PRS improves positioning accuracy. At high carrier-to-noise ratios, the number of transmitted PRS symbols have little influence on the accuracy performance, whereas increasing the sampling frequency can significantly enhance positioning accuracy. In addition, increasing the number of satellites used for positioning enhances the accuracy, whereas increasing the altitude of the satellites may degrade the accuracy. Moreover, the satellites deployment scenario has a noticeable impact on positioning accuracy. Finally, having imprecise knowledge of the satellites' positions, even by only a few meters, is observed to affect the accuracy substantially as well.

Popular Science Summary

Non-Terrestrial Network (NTN) is a network that includes non-terrestrial flying objects. High Altitude Platform Systems (HAPS), air-to-ground networks and satellite communication networks are all NTN systems. A satellite communication network, as illustrated in Fig. 1, uses satellites to communicate with one another, as well as with ground stations and User Equipment (UE). These satellites can be Low Earth Orbit (LEO) satellites, Medium Earth Orbit (MEO) satellites or Geostationary Earth Orbit (GEO) satellites. Nowadays, there is an interest in integrating satellite networks with 5G systems. NTN has the advantages of service continuity, scalability and availability, which will support 5G systems to achieve their challenging use cases. Service continuity means that the network can provide connection to UE at anytime and anywhere. Service scalability means that the network can maintain good service despite an increase in traffic load because of the support of NTN. Service availability means that the network is always available even in cases of disasters or similar situations. However, to facilitate these functionalities, the NTN needs to know the UE position.

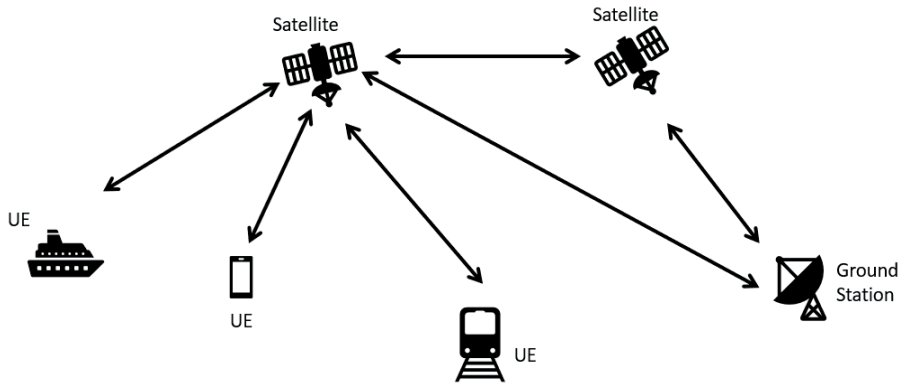

Fig. 1: NTN Satellite Communication

In 3rd Generation Partnership Project (3GPP) Release 17, UE positioning in NTN is performed with the existing Global Navigation Satellite System (GNSS). GNSS is a navigation satellite constellation that provides global or regional coverage and can be used for positioning purposes. Using GNSS in NTN has some drawbacks. Firstly, the UE device must have two separate receivers: one for positioning (GNSS receiver) and another one for

communication (NTN receiver). Secondly, the use of dual receivers may incur high power consumption at the UE. Therefore, it is highly desirable to extend the communication capability of NTN to enable positioning, so that the usage of GNSS is no longer required.

Observed Time Difference of Arrival (OTDOA) is one of the cellular positioning techniques that uses the time difference between the arrival of Positioning Reference Signals (PRS) for the computation of the location of the UE. In this thesis, an NTN simulator has been implemented in MATLAB using OTDOA as the positioning method. The NTN simulator is then used to investigate the appropriate PRS configuration in NTN. In addition, the impact of several factors on the positioning accuracy of the UE has been examined. It is shown that using OTDOA as the positioning method and PRS as the reference signal in NTN result in good positioning accuracy of within several meters. Moreover, it is shown that positioning accuracy varies depending on the channel model and satellite parameters used. Considering the satellite as a moving object, it is observed that inaccurate knowledge of the satellite locations results in substantial degradation of UE positioning estimation accuracy. For example, if the actual satellite positions are perturbed randomly from their nominal positions according to a zero mean normal distribution with a standard deviation of 2 meters, 50% of the UE will experience up to 50% more error in the estimated position.

Acknowledgments

I would like to thank my supervisors at Sony Research Center in Lund, Zhinong Ying and Basuki Priyanto for their supervision, feedback, and comments throughout the whole thesis work. Moreover, I would like to express my gratitude to my supervisor at Lund University, Prof. Buon Kiong Lau, for his continuous support and valuable advices. I am grateful as well to Zhang Yujie for his help and support in this thesis work. Finally, I want to thank my family for their love, support and encouragement during the whole masters' thesis project period.

Soha Emara

List of Acronyms

CNR	Carrier-to-Noise Ratio
C/A	Coarse/Acquisition
DL-AoD	Downlink Angle-of-Departure
DL-TDOA	Downlink Time-Difference-of-Arrival
GEO	Geostationary Earth Orbiting
GLONASS	GLObal NAvigation Satellite System
gNB	Next Generation NodeB
GNSS	Global Navigation Satellite System
GPS	Global Positioning System
HAPS	High-altitude Platform Station
HEO	Highly Elliptical Orbiting
IoT	Internet-of-Things
ISL	Inter Satellite Link
LEO	Low Earth Orbiting
MEO	Medium Earth Orbiting
MLE	Maximum Likelihood Estimator
Multi-RTT	Multi-cell Round Trip Time
MUSIC	MUltiple Signal Classification
M2M	Machine-to-Machine
NG-RAN	Next Generation-Radio Access Network
NR-Uu	New Radio air interface
NTN	Non-Terrestrial Network
OTDOA	Observed Time-Difference-of-Arrival
P code	Precise code
PRS	Positioning Reference Signal

RAT	Radio Access Technology
RSTD	Received Signal Time Difference
RTOA	Relative Time-of-Arrival
SRS	Sounding Reference Signal
TDOA	Time-Difference-of-Arrival
TMP	Transmission Measurement Function
TN	Terrestrial Network
TOA	Time-of-Arrival
UAS	Unmanned Aircraft System
UE	User Equipment
UL-AoA	Uplink Angle-of-Departure
UL-TDOA	Uplink Time-Difference-of-Arrival

Table of Contents

CHAPTER 1

Introduction

1.1 Background

The rapid progression in telecommunication technologies and the continuous increase in the number of smart devices over the last few decades have led to the necessity of non-terrestrial networks (NTNs). It is forecasted that the number of smartphones is expected to increase from 2018 to the end of 2024 by 45% and the amount of consumed data will increase by four times more than the consumed data in 2018, reaching 21GB on average per month [1]. Moreover, the fifth-generation (5G) wireless communication targets to have full coverage of the Earth. Therefore, NTN presents itself to be an effective solution for difficult 5G use cases that cannot be handled by terrestrial networks (TNs) alone. One such use case is to provide service for a user equipment (UE) in the middle of an ocean or a dessert.

An NTN is a network that uses satellites or Unmanned Aircraft System (UAS) platforms, instead of terrestrial base stations, to connect with UEs on the ground. According to the type of payload, be it regenerative or transparent, the payload acts as a base station or a repeater, respectively [2].

There are three main benefits from deploying NTNs. First, NTNs enable the TNs to extend their coverage areas to provide connectivity to previously unserved areas. In addition, NTNs can provide service availability in cases of disasters, where TNs may be damaged and hence cannot provide connectivity. Moreover, NTNs can provide service scalability to decrease the traffic load on the TNs [1].

1.2 Motivation

Nowadays, with the existence of 5G networks and their targeted data rate (of up to 20 Gbps) and reliability (up time of 99.999%), there are several service scenarios that arise where the UE needs to have multi-connectivity. Examples of such scenarios include the UE being in an underserved area, on board of an airplane or in a high-speed train. Multi-connectivity of the UE

can either be provided by simultaneous access to more than one NTN or by simultaneous access to a combination of TNs and NTNs [2]. The choice of the networks to connect depends heavily on the location of the UE. Accordingly, NTN positioning plays a vital role in multi-connectivity.

In the ongoing NTN standardization work within 3GPP Release 17, the assumption is to use the Global Navigation Satellite System (GNSS) as the positioning method. In this case, the NTN system has two receivers and its positioning functionality is dependent on GNSS. Moreover, using GNSS as a positioning method to complement NTN operation increases the power consumption at the UE. Therefore, it is highly desirable to remove GNSS and add a built-in positioning feature in NTN.

1.3 Goals

The overall purpose of this thesis is to investigate positioning techniques in an NTN consisting of a low earth orbit (LEO) satellite constellation in different configurations and deployment scenarios, based on which a suitable technique for NTN positioning may be proposed.

The objectives of this thesis are to:

- Find a feasible positioning signal and a suitable signal configuration for NTN positioning.
- Study the impact of different channels on positioning accuracy.
- Investigate the effect of satellite parameters on the performance.
- Analyse the impact of the uncertainty in the satellites' positions on the positioning accuracy of the proposed positioning technique.

In this thesis, the simulation tool is developed in MATLAB, partly based on the existing scripts that have been utilized to study positioning techniques for TNs.

1.4 Thesis Structure

The outline of this thesis is as follows: In Chapter 2, a brief introduction of NTN and 5G positioning techniques will be presented. In Chapter 3, a description for the simulated model will be given. In Chapter 4, the results from the simulator will be analysed. In Chapter 5, a summary for the thesis work and an outline for the future work will be given.

CHAPTER 2

Overview of NTNs and Positioning Systems

This chapter gives an overview of NTNs and positioning systems. Section 2.1 introduces NTN, its types and architecture. Section 2.2 describes satellite and cellular positioning systems.

2.1 Non-Terrestrial Networks

In this section, the first subsection gives a description of NTN. The second subsection presents the different types of platforms in NTN. The third subsection explains the NTN architecture based on Next Generation-Radio Access Network (NG-RAN) architecture.

2.1.1 NTN Description

NTN is a general term for any network that includes flying objects. Therefore, NTN includes satellite communication network and High-Altitude Platform station (HAPS). Satellite communication network uses spaceborne platforms for communication with the ground stations. HAPS are based on airborne Unmanned Aircraft System (UAS) platforms such as balloons and airships [3]. NTN uses RF resources on board an UAS platform or a satellite [2]. As shown in Fig. 2, an NTN typically consists of UAS platforms and/or satellites, one or several sat-gateways, feeder links, service links, inter satellite links (ISL) and UE [2]. The satellite or UAS platform implements either a transparent or a regenerative payload. For transparent payload, the waveform signal is frequency filtered, frequency converted and amplified. On the other hand, for regenerative payload, the waveform signal is frequency filtered, frequency converted and amplified as well as demodulated/decoded, switched and/or routed and coded/modulated. The sat-gateway connects the NTN to the data network. The feeder link is the link between the sat-gateway and the satellite or UAS platform whereas the service link is the link between the satellite or UAS platform and the UE. ISL is the link between satellites, in cases where more than one satellite is used [2].

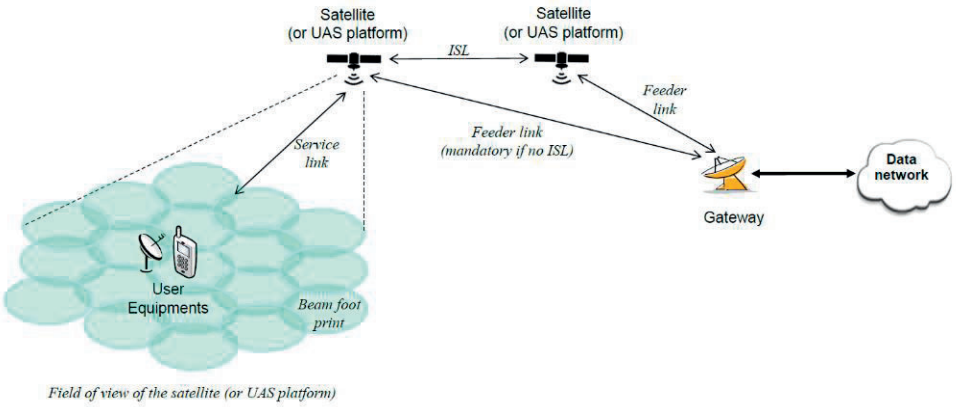

Fig.2: NTN based on regenerative payload [2]

2.1.2 Types of NTN platforms

There are five different types of satellites and UAS platforms that can be used in NTN. They are:

- Low Earth Orbiting (LEO) satellites
- Medium Earth Orbiting (MEO) satellites
- Geostationary Earth Orbiting (GEO) satellites
- UAS platform including High altitude Platform Station (HAPS)
- Highly Elliptical Orbiting (HEO) satellites

Each type has its own orbit, altitude range and beam footprint size. A GEO satellite orbits the Earth in a circular orbit at an altitude 35786 km. It appears motionless to Earth, as its orbital period is equal to the Earth's rotational period and its beam footprint size ranges between 200 - 3500 km. A MEO satellite orbits the Earth in a circular orbit at an altitude that ranges between 7000 - 25000 km and its beam footprint size ranges between 100 - 1000 km. A UAS platform has an altitude that ranges between 8 - 50 km and its beam footprint size ranges between 5 - 200 km. A HEO satellite rotates orbits the Earth in an elliptical orbit at an altitude ranges between 400 - 50000 km and its beam footprint size ranges between 200 - 3500 km. This thesis focuses on LEO satellites. A LEO satellite orbits the Earth in a circular orbit at an altitude that ranges between 300 - 1500 km and its beam footprint size ranges between 100 - 1000 km [2].

2.1.3 NTN Architecture

A NG-RAN can be adapted to support NTN in the case of using transparent or regenerative satellites. The transparent satellites act as RF repeaters. As shown in Fig. 3, it repeats the New Radio air interface (NR-Uu) from the feeder link to the service link and vice versa. Moreover, The NTN gateway has all the needed functions to forward the signal of NR-Uu interface. Therefore, the NG-RAN architecture is suitable to support transparent satellite access without the need for any modification. However, NR-Uu timers should be adapted to the long round trip times introduced in NTN [2].

The propagation delays in NTNs is much larger than those in TNs. In TNs, the propagation delay is less than 1 milliseconds. On the other hand, in NTNs, the propagation delay ranges from several milliseconds to hundreds of milliseconds. It is basically calculated as the distance between the satellite and the UE divided by the speed of light. Therefore, the propagation delays in NTNs strongly depend on the altitude of the satellite. Moreover, NTNs have large Doppler effects and moving cells. These issues point to the need for the modification of some timing parameters and enhancements of time and frequency synchronization [2].

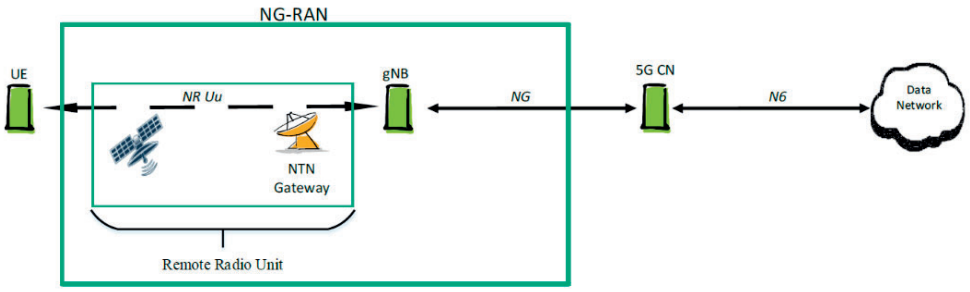

Fig. 3: NG-RAN architecture with transparent satellite [2]

2.2 Positioning methods

In general, the fundamental principle of positioning in cellular networks is having a terminal or a base station that performs signal measurements based on a transmitted reference signal. Using these measurements, the position of the UE is calculated using a certain algorithm. In the case of NTNs, the base station can instead be a satellite [4].

Positioning methods are divided into three main categories, which are UE-based, network-based and UE-assisted. In UE-based methods, the UE is responsible for calculating its own position by using signal measurements computed using signals from cellular or satellite transmitters. In network-based methods, the network location server is responsible for computing the location of the UE by using signal measurements carried out by the network with respect to the UE [4]. In UE-assisted methods, the location server is responsible for computing the position of the UE using signal measurements carried out by the UE [5].

Basically, computational techniques for UE positioning can be classified as multilateration, multriangulation, proximity, fingerprinting and hybrid [4]. In multilateration, the position of the UE is computed by calculating the distance between the reference transmitter and the UE and then finding the intersection between geometric forms. Time-of-Arrival (TOA) and Time-Difference-of-Arrival (TDOA) can be used in the measurements. In multriangulation, the position of the UE is estimated using the angle- or direction-of-arrival of the signals by finding the intersection of the directions of the received signals. In proximity, the location of the UE is estimated to be equal the location of the transmitter. In fingerprinting, the position of the UE is estimated by the best match to a location-specific signal measurement. Hybrid technique is a combination of more than one of the previous mentioned techniques.

In this section, a description of the existing satellite positioning solutions and cellular positioning solutions will be given.

2.2.1 Satellite Positioning Systems

A satellite positioning system is a satellite constellation that utilizes the signals broadcasted from satellites to measure the position of the receiver. A general term for a satellite positioning system is GNSS. GNSS is a navigation satellite constellation that provides global or regional coverage and can be used not only for positioning but for other purposes such as geology and geophysics [6]. There are different types of GNSS, for example Global Positioning System (GPS), Galileo, GLObal NAvigation Satellite System (GLONASS) and BeiDou [7]. Each of them has its own satellite constellation, coverage and accuracy. GPS is the most used GNSS as it is the oldest one, provides global coverage and is available in all counties [8].

In the following subsection, a detailed description of GPS and its positioning procedure will be discussed.

GPS Positioning

GPS consists of three segments: control segment, space segment and user segment. The control segment consists of a group of ground stations that control, monitor and track the satellites. The space segment composed of a satellite constellation that rotates around the Earth at a very high attitude. The user segment is the user equipment, it can be military or civilian equipment, that receive the GNSS signals [9].

As shown in Fig. 4, the GPS constellation consists of 24 operational satellites in 6 different orbital planes, covering the whole Earth. GPS satellites are MEO satellites, which orbit around the Earth in circular orbits at an altitude of approximately 20 200 km. It is designed in such a way that at least four satellites are seen simultaneously by users at any place on Earth [10].

Fig. 4: GPS Constellation

A GPS signal has two carrier signals, at the frequencies of 1575.42 MHz (L1) and 1227.60 MHz (L2), respectively. Each carrier signal is modulated by a combination of a navigation message and a code that is unique for each

satellite. The L1 carrier signal is modulated by two codes, which are coarse/acquisition (C/A) code and precise (P) code, whereas the L2 carrier signal is modulated by the P code only. The C/A code has a rate equal to 1.023MHz, repeats every 1 ms and has a wavelength of about 300 m. The P code has a rate that is 10 times higher than that of the C/A code, i.e., 10.23 MHz, repeats every 7 days and its wavelength is about 30 m. Therefore, P code is much more precise than the C/A code, and accordingly it is used for the military, whereas the C/A code is used for civilian purposes. The navigation message contains the data about the satellite position, velocity and time parameters. Its duration is 12.5 min and has a rate of 50 bits/s [9].

GPS satellites broadcast signals to GPS receivers that contain its three-dimensional position and the time the signal was sent. The time sent from the GPS satellites is accurate in comparison to the time observed at the receiver as the satellites have more stable clocks (i.e., atomic clocks) than the receivers. Once the signal is received, the receiver computes the time difference between the time the signal is sent and the time the signal is received. By knowing the time difference and the constant speed of radio waves (speed of light), the distance or the range between the transmitter (satellite) and the receiver (UE) can be calculated. In order for the receiver to be able to compute the four unknowns which are the three position coordinates and time, the receiver should receive signals from at least four satellites [11].

The atomic clocks of the satellites and the clock of the receiver are not precise. Therefore, the calculated range includes clock errors and it includes as well an extra delay resulting from the radio beam traveling through the Ionosphere and the Troposphere layers of the earth's atmosphere. Accordingly, the distance between the satellite and the receiver (R_i where i donates the i-th satellite) can be calculated by two methods. The first method is as follows [11]:

$$\mathrm{R}_i = \Delta \mathrm{t}_i \times \mathrm{C} \tag{2.1}$$

$$\Delta \mathrm{t}_i = \mathrm{Trec} - \mathrm{Tsent}_i + \mathrm{Tbias} - \mathrm{Terr}_i + \mathrm{Tatm}_i \tag{2.2}$$

where $\Delta \mathrm{t}_i$ is the path delay between the satellite and the UE, C is the speed of light, Trec is the receiver clock time when the signal is received, Tsent_i is the transmitter clock time when the signal is transmitted, Tbias is the

unknown receiver clock error, Terr_i is the satellite clock error and $\mathrm{Tatm}_i$is the extra delay resulting from the Earth's atmosphere change.

The second method to compute R_i is by using the distance formula as follows [11]:

$$\mathrm{R}_i = \sqrt{(\mathrm{X} - \mathrm{X}_i)^2 + (\mathrm{Y} - \mathrm{Y}_i)^2 + (\mathrm{Z} - \mathrm{Z}_i)^2} \tag{2.3}$$

where X, Y, Z are the user's coordinates and X_i, Y_i, Z_i are the satellite's coordinates.

Combining the two equations of R_i, we are left with four unknown parameters which are the UE longitude, latitude and altitude and the receiver clock bias. However, the equation set is nonlinear. Accordingly, one method to solve the equations is by linearizing the equations and using an iterative approach. In this method, initial assumed values for the user location and the user clock error are used and they are called nominal values. Moreover, delta terms are added to the nominal values to produce the actual values of the user location and the user clock error as follows [11]:

$$\mathrm{X} = \mathrm{X}_n + \Delta\mathrm{X} \tag{2.4}$$

$$\mathrm{Y} = \mathrm{Y}_n + \Delta\mathrm{Y} \tag{2.5}$$

$$\mathrm{Z} = \mathrm{Z}_n + \Delta\mathrm{Z} \tag{2.6}$$

$$\mathrm{Tbias} = \mathrm{Tb}_n + \Delta\mathrm{Tb} \tag{2.7}$$

where X_n, Y_n, Z_n are the user's nominal position, Tb_n is the nominal clock error and $\Delta\mathrm{X}$, $\Delta\mathrm{Y}$, $\Delta\mathrm{Z}$, $\Delta\mathrm{Tb}$ are the difference between the actual and the assumed values of the three user position coordinates and the receiver clock error respectively.

Using an iteration method, the delta terms can be computed. If the delta terms are equal to zero or have negligible values then it can be assumed that the actual and nominal values are equal. Otherwise, in case the delta terms are large then the delta terms will be added to the nominal values to form new nominal values. The process is repeated until small delta terms are reached [11].

The Pseudo-Range (PR_i) for each satellite can be calculated using equation (2.8). Pseudo-Range is the biased range between the satellite and the UE. In addition, the nominal Pseudo-Range (PR_n) is computed using equation 2.9 [11].

$$PR_i = \sqrt{(X - X_i)^2 + (Y - Y_i) + (Z - Z_i)^2} + Tbias \times C \quad (2.8)$$

$$PR_{ni} = \sqrt{(X_n - X_n)^2 + (Y_n - Y_i) + (Z_n - Z_i)^2} + Tbn \times C \quad (2.9)$$

Using the calculated nominal Pseudo-Range, the actual Pseudo-Range can be calculated as the sum of the assumed Pseudo-Range and the delta term [11]:

$$PR_i = PR_{ni} + \Delta PR_i \quad (2.10)$$

where PR_i is the difference between the actual and the estimated Pseudo-Range.

Combining equations (2.4) - (2.10), we will get, as shown in equation (2.11), *N* linear equations (*i* = 1, …, *N*) with four unknowns, which are ΔX, ΔY, ΔZ, ΔTb. All other terms are known or are estimated except for PR_i. Using the measured path delay, the ΔPR_i can be calculated [11].

$$\Delta PR_i = \alpha_{i1}\Delta X + \alpha_{i2}\,\Delta Y + \alpha_{i3}\,\Delta Z + C \times \Delta Tb \quad (2.11)$$

$$\alpha_{i1} = \frac{[X_n - X_i]}{PR_{ni} - Tb_n \times C} \quad (2.12)$$

$$\alpha_{i2} = \frac{[Y_n - Y_i]}{PR_{ni} - Tb_n \times C} \quad (2.13)$$

$$\alpha_{i3} = \frac{[Z_n - Z_i]}{PR_{ni} - Tb_n \times C} \quad (2.14)$$

Finally, the measured delta terms (ΔX, ΔY, ΔZ, ΔTb) must be examined. If they are small, then we can calculate the user position and receiver clock bias; else, we have to repeat the process until we reach acceptable small values for the delta terms [11].

2.2.2 Cellular Positioning Techniques in 5G TN

Cellular positioning techniques are methods that utilize the cellular communication infrastructure to compute the location of the UE. There are different types of RAT-dependent positioning solutions that are used in 5G NR, for example Downlink Time-Difference-of-Arrival (DL-TDOA), Uplink Time-Difference-of-Arrival (UL-TDOA), Multi-cell Round Trip Time (Multi-RTT), Uplink Angle-of-Arrival (UL-AoA) and Downlink Angle-of-Departure (DL-AoD). RAT-dependent means that the measurement techniques depend on the radio access technology.

Cellular signals have advantages over GNSS signals. First, they may provide higher received power. In addition, cellular signals have larger bandwidths than GNSS signals, which enhance Time-of-Arrival (TOA) estimation. Moreover, cellular signals are less susceptible to jamming and spoofing as they can be transmitted at different frequency bands [12]. On the other hand, GNSS signal includes important information for the receiver such as the satellite position and ionospheric model parameters. Furthermore, GNSS satellites have atomic clocks and accordingly the transmitted signals are well synchronized. In addition, cellular signals are not intended for positioning in the first place. Therefore, extracting the navigation and positioning information from them is complex [13].

In this subsection, a brief description for several RAT-dependent cellular positioning techniques will be given. A more detailed description of the DL-TDOA positioning technique and its reference signal will be provided as it is the positioning technique used in this thesis.

Uplink Time-Difference-of-Arrival

UL-TDOA is an uplink positioning method in 5G NR. In this method, the UE transmits a Sounding Reference Signal (SRS) to several gNBs. The measurement function for uplink techniques in 5G NR is known as the Transmission Measurement Function (TMF). The TMF calculates the Relative Time of Arrival (RTOA) and sends it to the location server in order

to compute the UE position according to the RTOA and the known geographical coordinates of the TMFs [14].

Multi-cell Round Trip Time

Multi-RTT is one of the standardized positioning solutions in 5G NR [5]. As shown in Fig. 5, the RTT is estimated using SRS and Positioning Reference Signal (PRS) transmitted and received between the UE and different gNBs. The location server computes the distance between the UE and the gNB using the measured RTT. Then, the UE position can be computed similar to other time-based techniques (DL-TDOA and UL-TDOA) utilizing trilateration algorithm. Multi-RTT has an advantage over other time-based techniques that there is no factor of the synchronization errors between the gNBs. However, the high cost of the multi-RTT is a drawback that has to be considered [14].

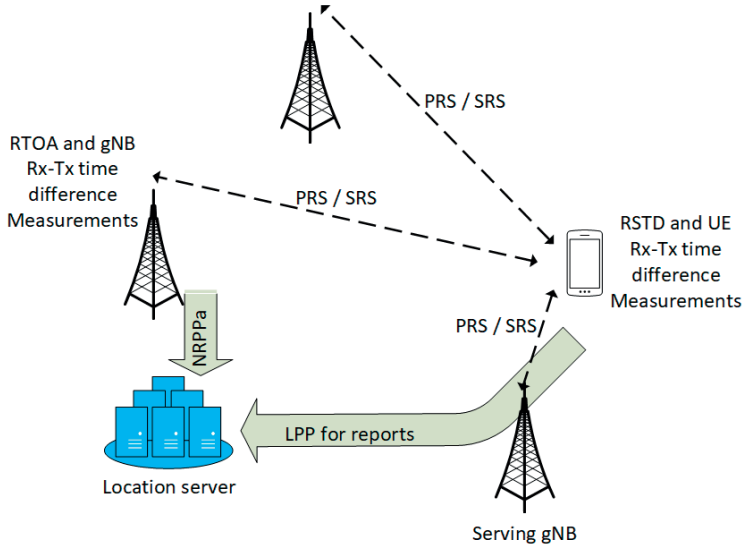

Fig. 5: Structure of multi-RTT positioning technique [14]

Uplink Angle-of-Arrival

UL-AoA is another positioning technique for 5G NR. As shown in Fig. 6, the AoA is measured using SRS at the gNBs in both the serving and neighbouring cells. After the location server receives the measured AoAs, it computes the location of the UE utilizing triangulation algorithm. AoA estimation can be performed by different methods for example the DFT beam method and the Multiple Signal Classification (MUSIC) method [14].

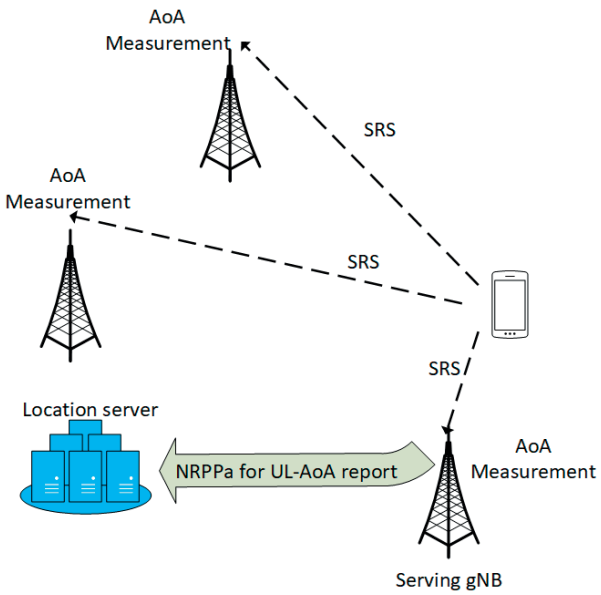

Fig. 6: Structure of UL-AoA positioning technique [14]

Downlink Angle-of-Departure

DL-AoD is a standardized positioning technique in NR [5]. Fig. 7 shows the structure of the DL-AoD. The AoDs from several gNBs are estimated using reference signal received power (RSRP) that is measured at the UE. One way to measure the RSRP is by utilizing the received PRS signals. After the location server receives the measured RSRP, it estimates the AoDs and computes the position of the UE utilizing triangulation. AoD estimation can be performed by different methods, for example by fingerprinting [14].

Downlink Time-Difference-of-Arrival

DL-TDOA is known as Observed Time-Difference-of-Arrival (OTDOA) [14]. It is one of the standardized downlink positioning solutions in 5G NR [5]. In this technique, the downlink signal is PRS. As shown in Fig. 8, the UE receives the PRS from several Next Generation NodeB (gNB) and calculates the TOA of each PRS signal. Afterwards, it considers one of the gNBs as a reference and computes Reference Signal Time Difference (RSTD) between the TOA of the signal from the reference gNB and the TOA of the other received signals from the other gNBs. UE sends the RSTD measurements to the location server in order to compute the UE position according to the RSTD and the known geographical coordinates of the gNBs. This technique needs at least three gNBs to get an accurate UE position [15].

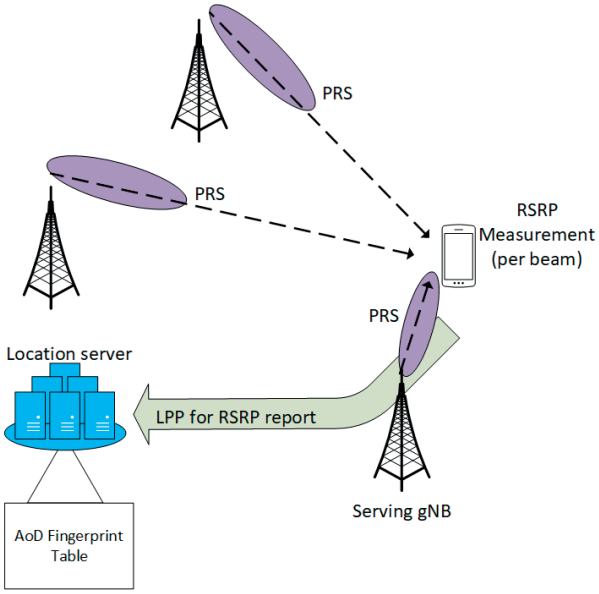

Fig. 7: Structure of DL-AoD positioning technique [14]

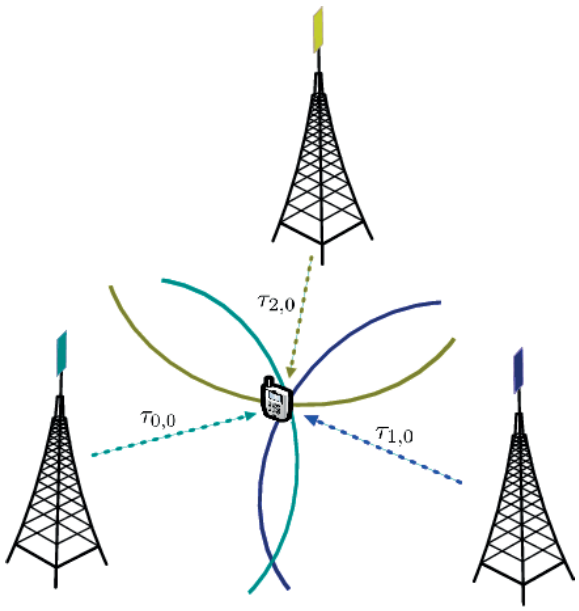

Fig. 8: OTDOA positioning [16]

Positioning Reference Signal

PRS is the DL reference signal used in the OTDOA technique. PRS is a pseudo-random sequence that is modulated by Quadrature Phase Shift Keying (QPSK). The pseudo-random sequence used is a Gold sequence of length 31. The reference signal sequence $r(m)$ generated by the UE is as follows [16]:

$$r(m) = \frac{1}{\sqrt{2}}\big(1 - 2c(2m)\big) + j\frac{1}{\sqrt{2}}\big(1 - 2c(2m+1)\big) \qquad (2.15)$$

The pseudo-random generator $c(m)$ is initialized as follows [17]:

$$c_{\text{init}} = (2^{22}\left\lfloor \frac{n_{\text{ID,seq}}^{\text{PRS}}}{1024} \right\rfloor + 2^{10}\big(N_{\text{symb}}^{\text{slot}} n_{\text{s,f}}^{\mu} + l + 1\big)\big(2\big(n_{\text{ID,seq}}^{\text{PRS}} \bmod 1024\big) + 1\big) + \big(n_{\text{ID,seq}}^{\text{PRS}} \bmod 1024\big)) \bmod 2^{31} \qquad (2.16)$$

where $n_{\text{ID, seq}}^{\text{PRS}} \in \{0,1, \ldots, 4095\}$ is the downlink PRS sequence ID, $N_{\text{symb}}^{\text{slot}}$ is the number of symbols per slot, $n_{\text{s, f}}^{\mu}$ is the slot number and l is the OFDM symbol where the sequence is allocated.

Each PRS is then scaled by a factor (β_{PRS}) and allocated to certain resource elements as follows [17]:

$$a_{k,l}^{(p,\mu)} = \beta_{\text{PRS}}\, r(m) \qquad (2.17)$$

$$k = mK_{\text{comb}}^{\text{PRS}} + \Big(\big(k_{\text{offset}}^{\text{PRS}} + k'\big) \bmod K_{\text{comb}}^{\text{PRS}}\Big)\; m = 0, 1, \ldots \qquad (2.18)$$

$$l = l_{\text{start}}^{\text{PRS}}, l_{\text{start}}^{\text{PRS}} + 1, \ldots, l_{\text{start}}^{\text{PRS}} + L_{\text{PRS}} - 1 \qquad (2.19)$$

where k and l together represent the resource element where k is the subcarrier number and l is the OFDM symbol number. $l_{\text{start}}^{\text{PRS}}$ is the first OFDM symbol of the downlink PRS in a slot. L_{PRS} is the number of symbols that contain PRS resources. $K_{\text{comb}}^{\text{PRS}} \in \{2, 4, 6, 12\}$ is the comb size and $k_{\text{offset}}^{\text{PRS}}$ is the resource element offset.

Table 2.1: The frequency offset k' as a function of $l - l_{\text{start}}^{\text{PRS}}$ [17].

$K_{\text{comb}}^{\text{PRS}}$	Symbol number within the DL PRS resource $l - l_{\text{start}}^{\text{PRS}}$											
	0	**1**	**2**	**3**	**4**	**5**	**6**	**7**	**8**	**9**	**10**	**11**
2	0	1	0	1	0	1	0	1	0	1	0	1
4	0	2	1	3	0	2	1	3	0	2	1	3
6	0	3	1	4	2	5	0	3	1	4	2	5
12	0	6	3	9	1	7	4	10	2	8	5	11

CHAPTER 3

Simulation Methodology

In this chapter, a description for the implemented simulator will be given in detail. Section 3.1 demonstrates the full procedure of the simulator. Section 3.2 introduces the satellite constellation. Then, Section 3.3 describes the antenna model, and Section 3.4 defines the Doppler shift and delay. Next, Section 3.5 defines the path loss and SNR, and Section 3.6 illustrates the receiver. Finally, Section 3.7 describes the channel model.

3.1 Simulation Procedure

In this section, the implemented simulator is described. Fig. 9 shows a block diagram of the simulator procedure. In the beginning, UEs are dropped randomly in an area that is covered by several satellites. In this area, the elevation angle between each UE and each satellite ranges from 30 degree to 90 degree. Then, the satellites broadcast the reference positioning signals to all UEs. This is followed by the calculation of the channel coefficients and the application channel effects. Two channel models are built into the simulator, which are large-scale fading model and fast-fading model. The effect of path loss and shadow fading are also added and the Carrier-to-Noise Ratio (CNR) is calculated. In addition, a White Gaussian Noise (WGN) is added to the signal.

The UE receives the transmitted signal after the channel is applied, and it computes the correlation between the received signal and the reference signal. Then, it calculates the TOA of the first path using a threshold-based method. Finally, the location server computes the estimated position of the UEs using Maximum Likelihood Estimator (MLE).

3.2 Satellite Constellation

The reference satellite constellation used is Starlink Phase I constellation. This constellation provides internet service with high speed and low latency to the users all over the world, even in underserved areas. This makes it one of the more interesting constellations today. The Starlink Phase I

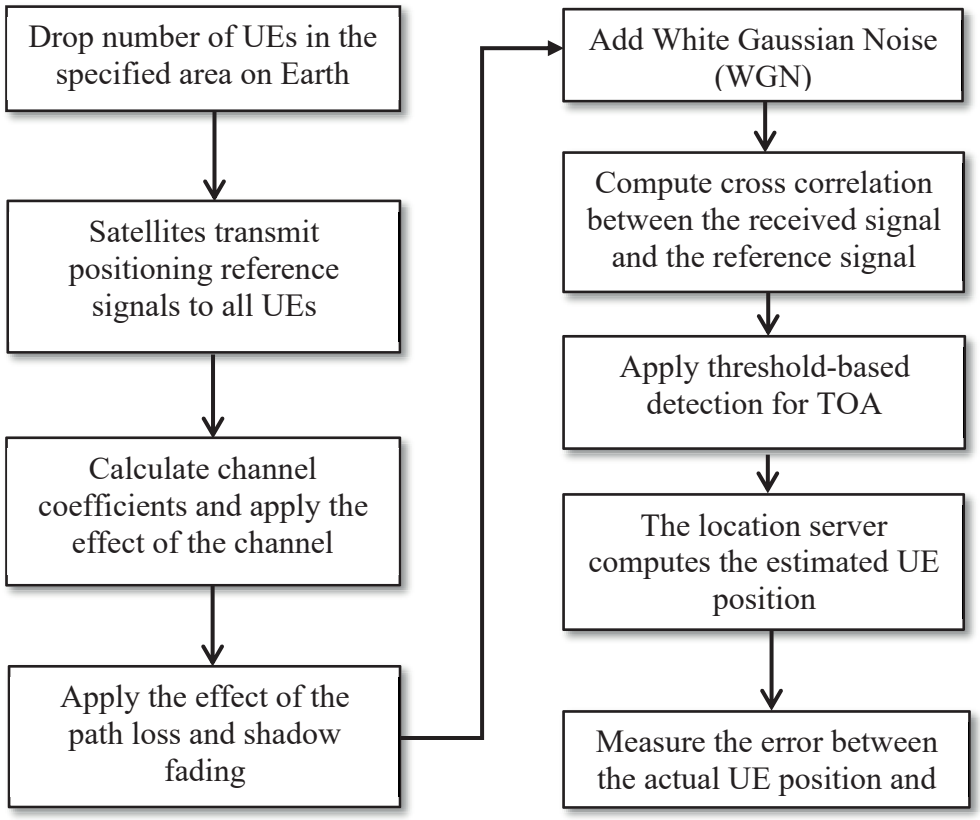

Fig. 9: Simulator Procedure

constellation, as shown in Fig. 10, consists of 24 planes. There are 66 satellites in each plane, giving in total 1584 satellites that cover the whole Earth. The satellites are LEO satellites at an altitude of 550 km. The orbits are inclined by 53º with respect to the Equator while the orbital planes spacing is equal to 15º [18].

The simulations in this thesis focus on a certain area on Earth. This area has the form of a circle, with a radius that is equal to 850 km, as depicted in Fig. 11. This area is covered by 9 satellites in two different orbits. The 9 satellites are divided into 5 satellites in the first orbit and 4 satellites in the second orbit. The first orbit is inclined by 2º, whereas the second orbit is inclined by 17º.

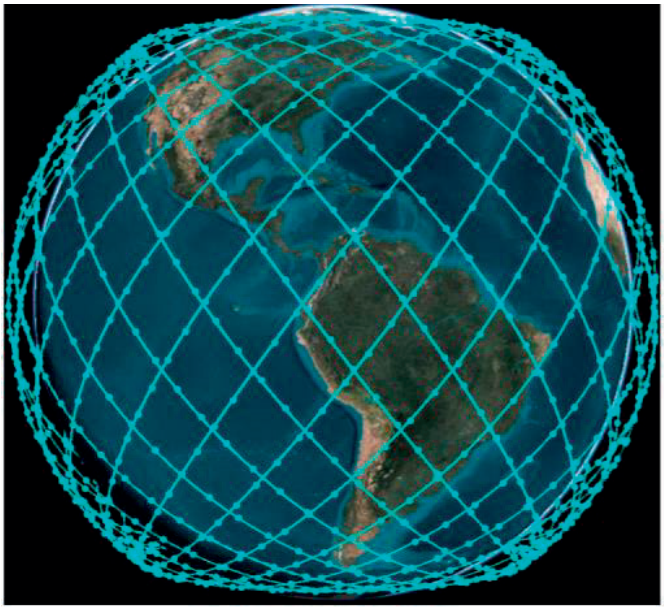

Fig. 10: StarLink Phase I Constellation [18]

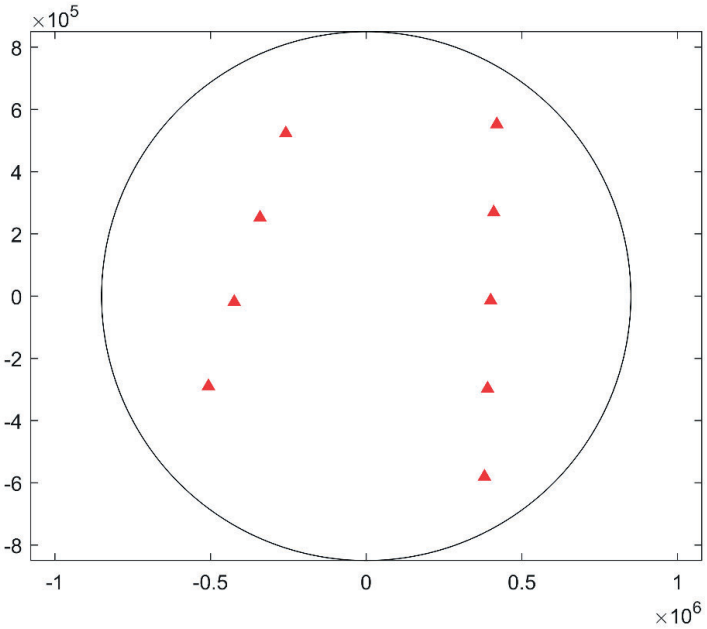

Fig. 11: The layout of the area on Earth

Following [2], each satellite transmits 19 beams, forming 19 beam footprints on Earth as shown in Fig. 12. In this simulator, the frequency reuse factor is 1 which means that the whole system frequency bandwidth is used in all beam footprints. The beam pattern is moving with the movement of the satellite.

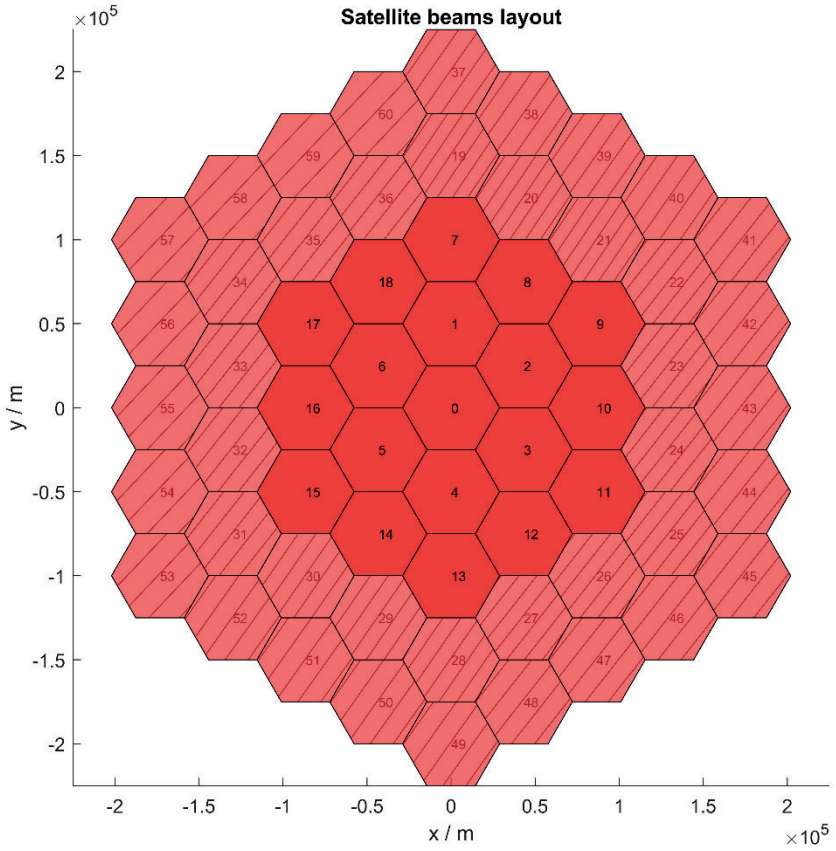

Fig. 12: Satellite Beam Pattern

3.3 Antenna Model

In this thesis, the satellites antenna model is a S-band reflector antenna with a circular aperture, which has a normalized antenna gain as follows [19]:

$$1 \qquad for\ \theta = 0 \tag{3.1a}$$

$$4\left|\frac{J_1(ka\ \sin\theta)}{ka\ \sin\theta}\right|^2 \qquad for\ 0 < |\theta| < 90° \tag{3.1b}$$

where $J_1(ka\ \sin\theta)$ is the Bessel function of the first order and first kind of the argument $ka\ \sin\theta$. k is the wavenumber, a is the radius of the antenna's aperture and θ is the angle calculated from the bore sight of the antenna's main beam.

The satellite antenna used has the maximum transmit antenna gain of 30 dBi, a is equal to 10 wavelengths, the 3 dB beamwidth is 4.4127º. Its normalized gain pattern is shown in Fig. 13.

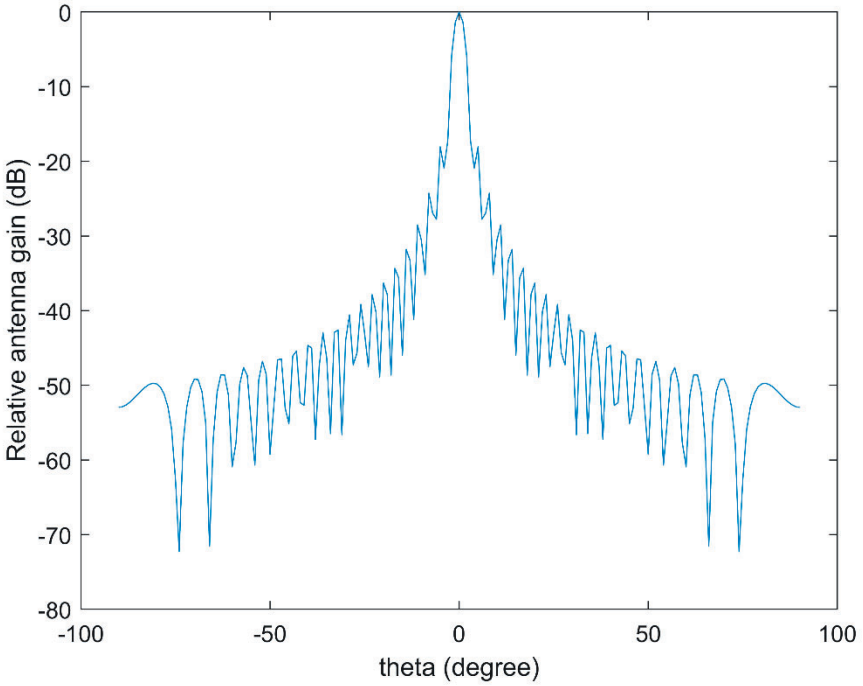

Fig. 13: Relative antenna gain for an aperture radius = 10 wavelengths

The UE use case is a S-band handheld case with an omnidirectional antenna that is linearly polarized. The transmit and receive antenna gains are 0 dBi.

3.4 Doppler Shift and Delay

In NTNs, there are high Doppler shifts due to the satellite movement and the UE movement, which lead to a frequency offset in the received signal. The frequency offset (FO) is calculated as follows [2]:

$$FO = (A_{UE} + DS_{Sat} + DS_{UE}) \times 10^{-6} \times f_c \quad (3.2)$$

where A_{UE} is the UE crystal accuracy, DS_{Sat} is the Doppler shift due to satellite movement, DS_{UE} is the Doppler shift due to the UE movement and f_c is the carrier frequency. In this simulation, A_{UE} is equal to 10ppm, DS_{Sat} is the maximum Doppler shift for a LEO satellite at the specified height, as shown in Table 3.1, f_c = 2 GHz (S-band) and DS_{UE} is calculated as follows [19]:

$$DS_{ue} = f_c \times V \times cos\,\theta/c \quad (3.3)$$

where V is the UE velocity, θ is the angle between the velocity vector of the UE and the direction of propagation of the signal between the UE and the satellite and *c* is the speed of light.

Table 3.1 shows the maximum propagation delay between a LEO satellite at different altitudes and a UE at 10º elevation angle. The propagation delays in NTNs are much larger than in TNs. It differs according to the altitude of the satellite. For LEO satellites, the propagation delay is in the range of several milliseconds [2].

Table 3.1: Maximum Delay and Doppler Shift for LEO satellite at different altitudes [2].

Altitude / Parameters	**LEO at 600 km**	**LEO at 1200 km**
Delay	6.44 ms	10.44 ms
Doppler Shift	+/- 48 kHz	+/- 42 kHz

3.5 Path Loss and CNR

The signal transmitted from the satellite to the UE is attenuated due to its propagation in space. This attenuation is modeled as the free space path loss (PL_{FS}) and is calculated in dB as follows [19]:

$$\mathrm{PL}_{FS} = 20\ \log_{10}(\mathrm{d}) + 20\log_{10}(\mathrm{f}_c) - 147.55 \qquad (3.4)$$

where d is the distance between the satellite and the UE in meters and f_c is the carrier frequency in GHz.

In NTNs, CNR is calculated in dB as follows [2]:

$$\mathrm{CNR} = \mathrm{EIRP} + \frac{\mathrm{G}}{\mathrm{T}} - \mathrm{k} - \mathrm{PL}_{FS} - \mathrm{PL}_{A} - \mathrm{PL}_{SM} - \mathrm{PL}_{SL} - \mathrm{PL}_{AD} - \mathrm{B} \qquad (3.5)$$

where EIRP is the effective radiated isotropic power, $\frac{G}{T}$ is the antenna gain to noise temperature, k is Boltzmann constant, PL_A is the atmospheric path loss, PL_{SM} is the shadowing margin, PL_{SL} is the scintillation loss, PL_{AD} represents any additional loss and B is the channel bandwidth.

3.6 UE Receiver

The UE, which is the receiver, is a handheld 5G NR device that has an omnidirectional antenna, with the receive antenna gain of 0 dBi at S-band and the noise figure of 7 dB. The UE calculates the TOA of the reference signal sent from the satellite to the UE, to be used in the estimation of its position. In this thesis work, the positioning method used is based on OTDOA method and the satellites and UEs are time synchronized.

First, the UE computes the cross correlation between the reference signal sent from the satellite and the signal received by the UE. The correlator used is a frequency domain correlator as it reduces the computation complexity in comparison with a time domain correlator. Then, the output from the correlator is the input to the peak detector. In the peak detector, the signal arrival region is firstly detected. Then, the noise floor is estimated. This is followed by the use of a threshold-based method in the arrival region to estimate the delay of the first path using the noise floor and the output from the correlator. The thresholding method is illustrated in Fig. 14, in which the threshold is equal to 0.6.

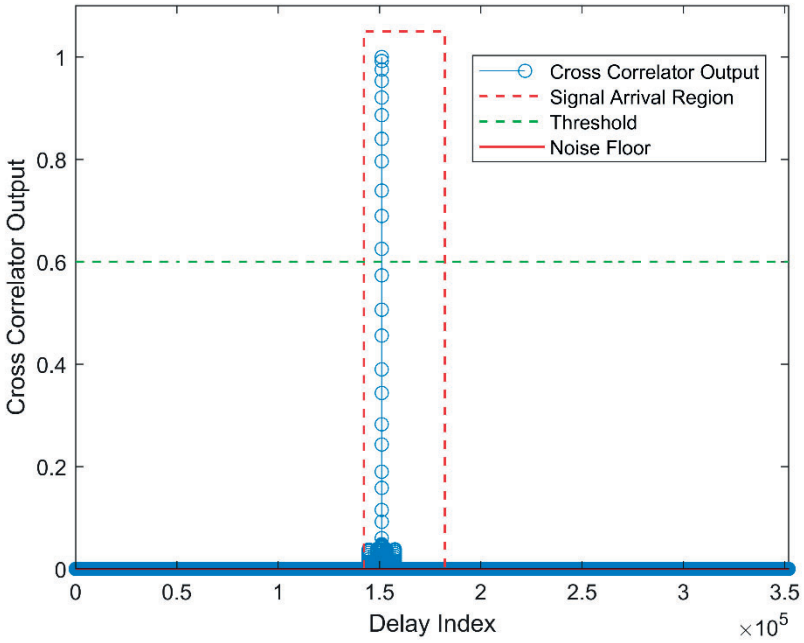

Fig. 14: An example for the threshold-based first path detection

Finally, the location server can estimate the UE location using the estimated TOA and the satellites' positions. The algorithm used by the location server in this simulation is maximum likelihood algorithm.

3.7 Channel Model

In this thesis, two channel models are examined. Firstly, a LOS large-scale fading channel is implemented. In this model, the fading parameters are path loss and shadow fading, and there is only one path (LOS path). Secondly, a frequency selective channel model is implemented based on the procedure mentioned in 3GPP TR 38.900 [20]. This procedure is the same as in the case of TNs but different channel parameters are used. These parameters depend on the presence of LOS path, frequency band and deployment scenario. In this thesis, the scenarios tested are rural and dense urban deployment scenarios in S-band. Some of the channel parameters used for rural and dense urban deployments are highlighted in Tables 3.2 and 3.3 respectively. The rest of the channel parameters can be found in 3GPP TR 38.811 [19]. In NTNs, the channel parameters change according to the elevation angle between the satellite and the UE, as shown in Table 3.2 and 3.3.

Table 3.2: Channel parameters for Rural deployment in S-band [19].

Elevation angle	Probability of LOS	**LOS** Shadow Fading (dB)	**LOS** Clutter Loss (dB)	**NLOS** Shadow Fading (dB)	**NLOS** Clutter Loss (dB)
10º	78.2%	1.79	0	8.93	19.52
20º	86.9%	1.14	0	9.08	18.17
30º	91.9%	1.14	0	8.78	18.42
40º	92.9%	0.92	0	10.25	18.28
50º	93.5%	1.42	0	10.56	18.63
60º	94.0%	1.56	0	10.74	17.68
70º	94.9%	0.85	0	10.17	16.50
80º	95.2%	0.72	0	11.52	16.30
90º	99.8%	0.72	0	11.52	16.30

Table 3.3: Channel parameters for Dense Urban deployment in S-band [19].

Elevation angle	Probability of LOS	**LOS** Shadow Fading std (dB)	**LOS** Clutter Loss (dB)	**NLOS** Shadow Fading std (dB)	**NLOS** Clutter Loss (dB)
10º	28.2%	3.5	0	15.5	34.3
20º	33.1%	3.4	0	13.9	30.9
30º	39.8%	2.9	0	12.4	29.0
40º	46.8%	3.0	0	11.7	27.7
50º	53.7%	3.1	0	10.6	26.8
60º	61.2%	2.7	0	10.5	26.2
70º	73.8%	2.5	0	10.1	25.8
80º	82.0%	2.3	0	9.2	25.5
90º	98.1%	1.2	0	9.2	25.5

CHAPTER 4

Performance Evaluation

In this chapter, the simulation results for NTN positioning accuracy will be presented and discussed. The horizontal positioning accuracy was evaluated for different cases and configurations. Section 4.1 shows the impact of PRS configuration. Then, Section 4.2 explains the impact of different satellite parameters. Section 4.3 demonstrates the effect of the channel model on the performance. Finally, Section 4.4 discusses the influence of uncertainty in the satellites' positions.

Table 4.1 lists the default simulation parameters for the considered NTN. It will be stated in the following sections if any of these parameters is changed to evaluate the impact of a specific parameter.

Table 4.1: Default simulation parameters.

Number of UEs	1000 UEs
Number of satellites	9 satellites
Satellite altitude	600 km
Channel model	Large-scale fading LOS model
Carrier frequency	2 GHz (S-band)
Bandwidth	2.16 MHz
Subcarrier spacing	15 kHz
K-comb	2
Number of PRS symbols per slot	2
Number of slots	1

4.1 Impact of PRS Configuration

Simulation results were obtained for different PRS configurations. Firstly, the horizontal positioning accuracy was evaluated for different bandwidths. Secondly, the accuracy was studied for different sampling rates. Finally, the accuracy was examined for different numbers of PRS symbols per slot. In

the following subsections, the results for each case will be presented and discussed in detail.

4.1.1 Channel Bandwidth

In these simulations, the system was evaluated with two different channel bandwidths. In the first simulation, the default parameters were used, in which the bandwidth was equal to 2.16 MHz. In the second simulation, the bandwidth used was 4.32 MHz, the subcarrier spacing was 30 kHz, the number of slots was 2 and the rest of the parameters followed the default parameters in Table 4.1. The simulation results for different bandwidths are presented in Fig. 15. It shows that with the increase of the bandwidth, the performance has improved. The positioning error is less than 3 m for 86% of the UEs, when the bandwidth was 2.16 MHz. On the other hand, the positioning error is less than 3 m in 99% of the UEs, when the bandwidth was increased to 4.32 MHz.

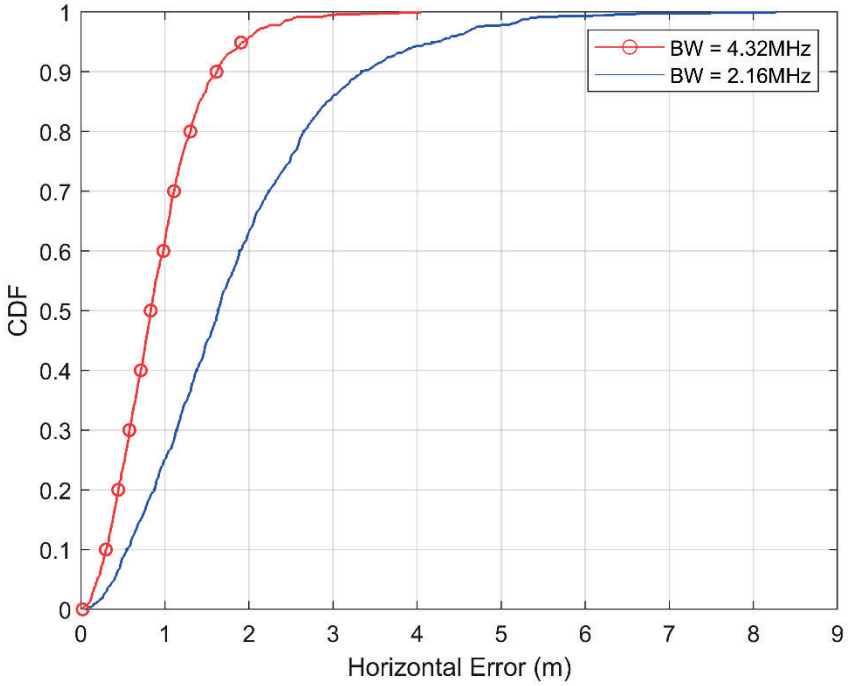

Fig. 15: Horizontal positioning accuracy with different bandwidths

This improvement was expected because the increase of the bandwidth is a result of the increase in the subcarrier spacing. Consequently, the number of

slots transmitted during the same time period (of 1 ms) are doubled, which means higher number of PRS transmitted per unit time. The time slot in case of subcarrier spacing equals 15 kHz is 1 ms while in case of 30 kHz subcarrier spacing the slot time is 0.5 ms. Having more PRS symbols enhances the channel estimation and therefore positioning accuracy. Moreover, the increase of the subcarrier spacing leads to an increase in the sampling frequency. The sampling frequency in the case of 15 kHz subcarrier spacing is 61.44 MHz whereas in the case of 30 kHz subcarrier spacing, it is equal to 122.88 MHz. This increase in the sampling frequency leads to an improvement in the resolution of the channel estimation and therefore, more accurate TOAs can be computed resulting in higher positioning accuracy.

In the following simulations, the effects of the sampling rate and the number of PRS symbols per unit time were investigated separately, to evaluate their respective contributions to the accuracy performance.

4.1.2 Sampling Frequency

To clearly examine the effect of the sampling frequency, the number of PRS symbols per unit time was fixed. In the first simulation, the subcarrier spacing was 15 kHz, the sampling frequency was 61.44MHz and bandwidth was 2.16MHz. In the second simulation, the subcarrier spacing was 30 kHz, the sampling frequency was 122.88 MHz and bandwidth was 8.64 MHz.

The results of horizontal positioning accuracy for using different sampling rate are shown in Fig. 16. It is shown that by increasing the sampling frequency, the performance is improved. The positioning error is less than 3 m in 86% of the UEs in the case of the sampling frequency being 61.44 MHz. On the other hand, the positioning error is less than 3 m in 99% of the UEs in the case of sampling frequency being 122.88 MHz.

These results show that a better performance can be achieved despite of having same number of PRS symbols per slot and number of resource elements occupied by PRS. Furthermore, the accuracy improvement with higher sampling frequency is practically the same as that in Fig. 15. Therefore, the sampling frequency has the dominant impact on the accuracy performance and that the performance of the previous simulation was mainly affected by the sampling rate rather than the number of PRS symbols.

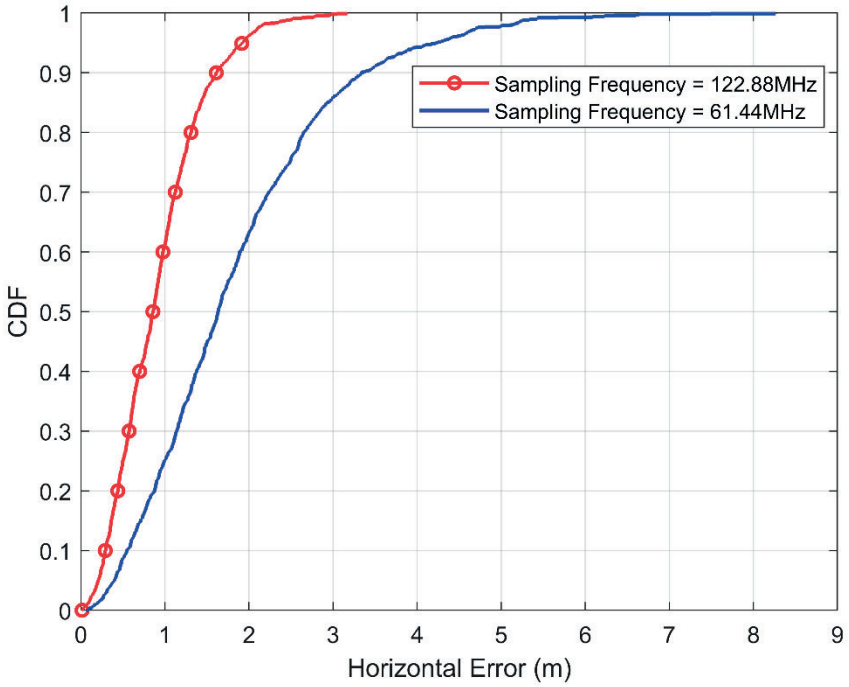

Fig. 16: Horizontal positioning accuracy for different sampling frequencies

To further validate the dominant effect of the sampling rate on the performance, the impact of using different number of PRS symbols per slot is examined in the next simulation (while keeping sampling frequency constant).

4.1.3 Number of PRS Symbols per Slot

In these simulations, the effect of the number of transmitted PRS symbols per slot was tested. The simulations were done for 2, 4 and 12 PRS symbols per slot. All other parameters followed the default parameters listed in Table 1. The results for these simulations are shown in Fig. 17. The positioning error is less than 4 m in 94% of the UEs in the case of 2 PRS symbols, whereas it is less than 4 m in 96% of the UEs in the case of 4 PRS symbols equals 4, and it is less than 4 m in 97% of the UEs in the case of 12 PRS symbols.

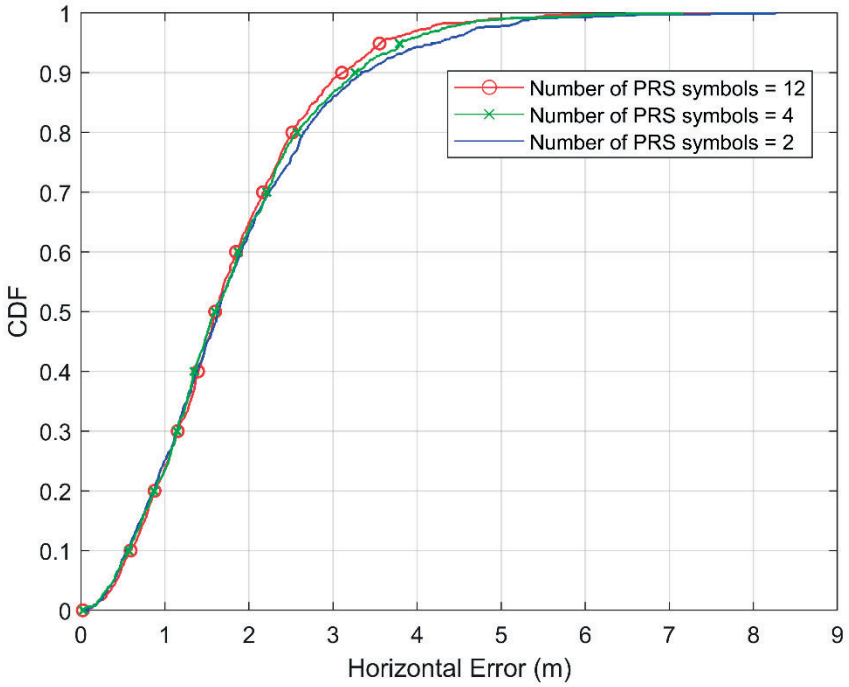

Fig. 17: Horizontal positioning accuracy for different number of PRS symbols

Therefore, there are only slight differences in the results for the 3 cases. The reason for this behaviour is the high CNR in the NTN downlink system. According to [2], the UE has the CNR of 6.6 dB, for the case study involving a LEO satellite at 600 km altitude in S-band, a handheld UE, 30 MHz system bandwidth and 30º elevation angle between the satellite. In the simulations performed in this thesis, the considered bandwidth is much smaller, which leads to a further increase in the CNR according to equation (3.5). Moreover, the calculated elevation angle between the satellite and the UE is in range of 30º~90º. As the elevation angle increases, the distance between the satellite and UE decreases resulting in a decrease in the path loss and an increase in the CNR. As shown in Fig. 18, the calculated CNR for the simulated UEs is in the range of 8.1-17.1 dB.

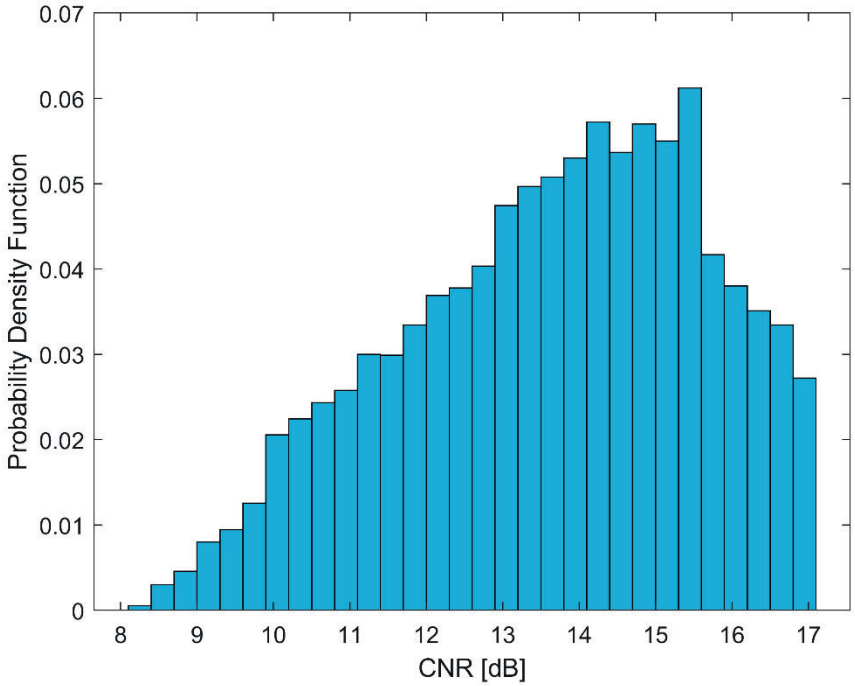

Fig. 18: The probability density function of the received signal CNR.

Normally, increasing the number of transmitted PRS symbols per slot results in better cross correlation between the received signal and reference signal. Consequently, the system becomes more resistant to noise and better positioning accuracy is achieved. However, in this simulated NTN study, the effect of increasing the number of PRS symbols is not as noticeable because the CNR is high.

4.2 Impact of Satellite Configuration

The simulation results for different satellite configurations were obtained. In the following subsections, the impact of the number of satellites used to compute the UE position is analysed. Then, the impact of the satellite altitude is discussed.

4.2.1 Number of Satellites

In these simulations, each of the 1000 UEs chose the same number of satellites to be used in computing its position. All the UEs chose either 5 or 9 satellites. All other parameters used in these simulations were the default

parameters given in Table 4.1. The distribution of the 9 satellites along 2 orbits is shown in Fig. 11, and the case of 5 satellites is based on randomly choosing (with equal probability) 5 of the 9 satellites.

It is shown in Fig. 19 that the positioning error is 2.6 m in 80% of the UEs in the case of using 9 satellites. On the other hand, the positioning accuracy is 4.5 m in 80% of the UEs in the case of using 5 satellites.

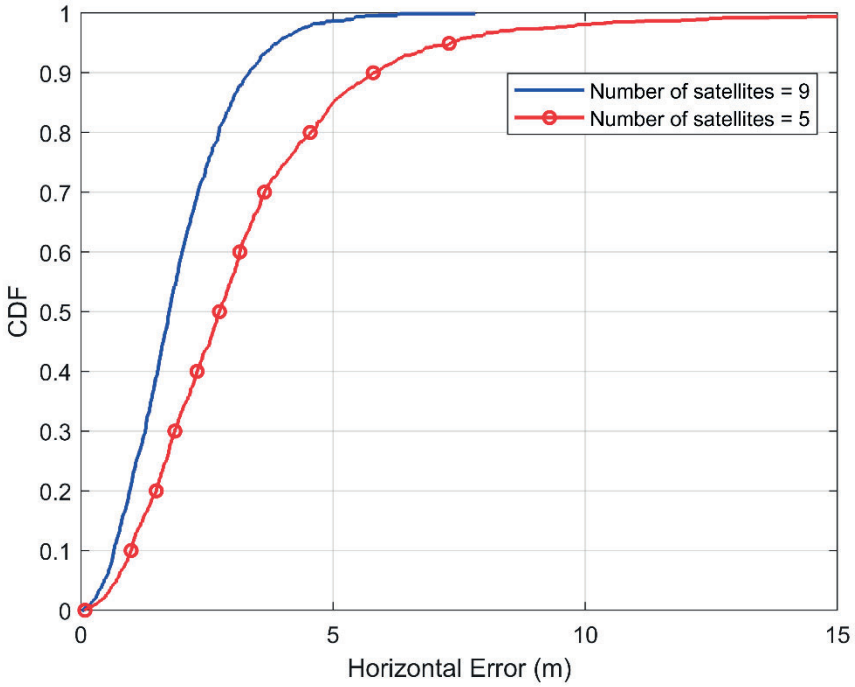

Fig. 19: Horizontal positioning accuracy for different number of satellites

The use of 9 satellites significantly outperforms the use of 5 satellites, in terms of positioning accuracy. This is because randomly choosing 5 satellites may result in the satellites of the same orbit being chosen. In this case, the performance of the positioning algorithm degrades, as it is based on the multilateration method. Moreover, increasing the number of satellites gives the algorithm more data to perform positioning. Consequently, the algorithm could give a more accurate position for the UE for the 9-satellite case.

4.2.2 Satellite Altitude

Two different satellite altitudes were tested in the simulations. The parameters that are affected by the change in the satellite altitude are the transmit power, path loss, CNR, Doppler shift and speed. The parameters used for the two cases of satellite altitude are shown in Table 4.2. Fig. 20 shows the corresponding simulation results. The positioning error is less than 4 m in 83% of the UEs in the case of using the satellite altitude of 1200 km. On the other hand, the positioning accuracy is less than 4 m in 94% of the UEs in the case of using the satellite altitude of 600 km.

Table 4.2: Satellite Altitude Parameters.

Altitude / **Parameters**	**600km**	**1200km**
Satellite EIRP density (dBW/MHz)	34	40
Doppler Shift (ppm)	24	21
Speed (km/s)	7.56	7.26
Path Loss	Lower	Higher

Although satellites at the altitude of 1200 km have higher path loss as the distances between the satellites and UEs have increased, the transmit power has been increased as well, which compensates the CNR. Therefore, the CNR is similar in both cases. However, it is observed that as the altitude of the satellite increases, the positioning error increases. For example, if the error in distance (the distance between satellite and UE) is same for a satellite at 600 km and a satellite at 1200 km, the timing error (the difference between the correct TOA and the estimated TOA) is same for a satellite at 600 km and a satellite at 1200 km. Then, from a geometric point of view, having a higher altitude will result in a larger error in the estimated x-y dimensions.

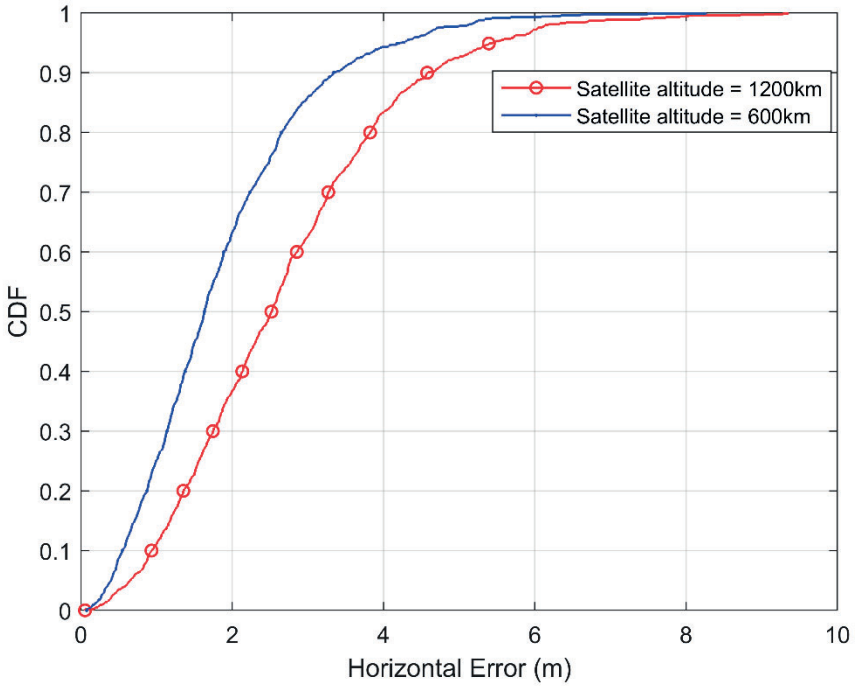

Fig. 20: Horizonal positioning accuracy for different satellite altitude

4.3 Impact of Channel Models

In these simulations, the impact of the fast-fading channel model is examined based on the parameters previously mentioned in Section 3.7 for two different scenarios. The first deployment scenario is rural scenario, and the second deployment scenario is dense urban scenario. As shown in Fig. 21, rural scenario has better performance than dense urban scenario. The positioning error is less than 5.5 m in 80% of the UEs in rural scenario while it is less than 16 m in 80% of the UEs in dense urban scenario.

CNR is lower in case of NLOS channels than in LOS channels. As mentioned before in Tables 3.2 and 3.3, the signal is affected by the shadow fading and the clutter loss in NLOS channels. However, there is no clutter loss in LOS channels. Moreover, the dense urban scenario has a higher probability of NLOS than rural scenario. In addition, the dense urban scenario has a larger shadow fading standard deviation than the rural scenario, as shown in Fig. 22. The probability density function of CNR plotted in Fig. 23 is based on

samples taken from 9000 simulated received signals. It shows that the rural scenario has an overall higher CNR than the dense urban scenario. Having higher CNR means higher received power and consequently higher positioning accuracy.

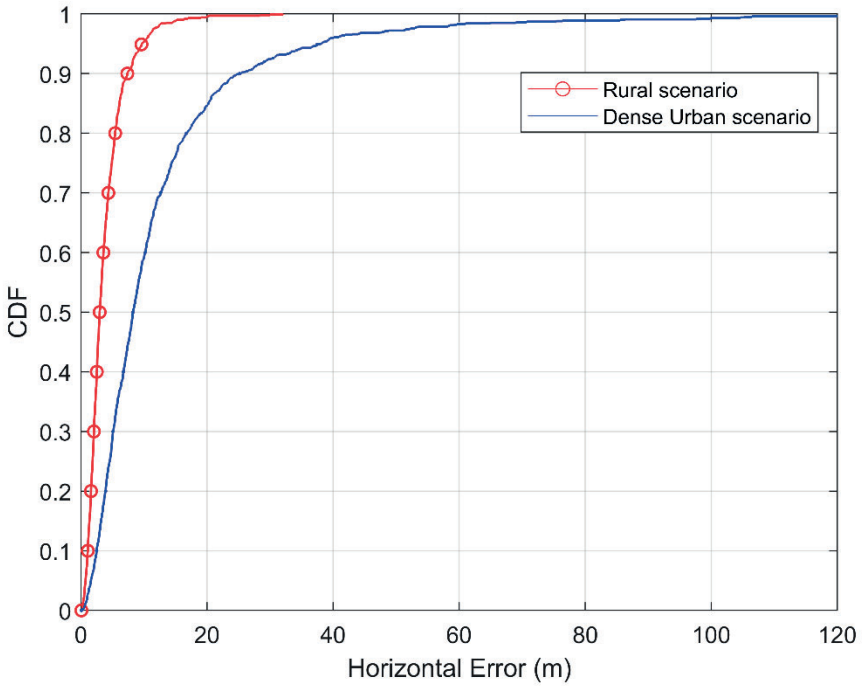

Fig. 21: Horizonal positioning accuracy for different deployment scenarios

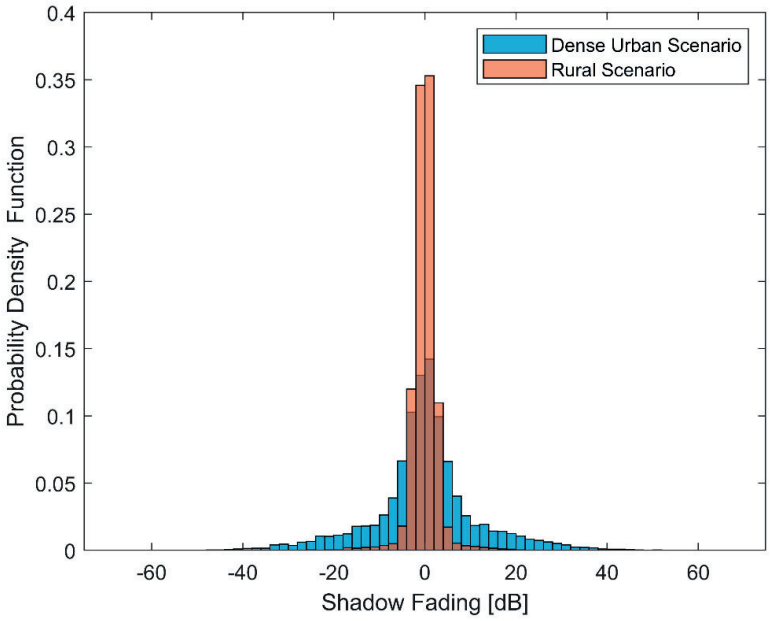

Fig. 22: The probability density function for the shadow fading in rural and dense urban scenarios

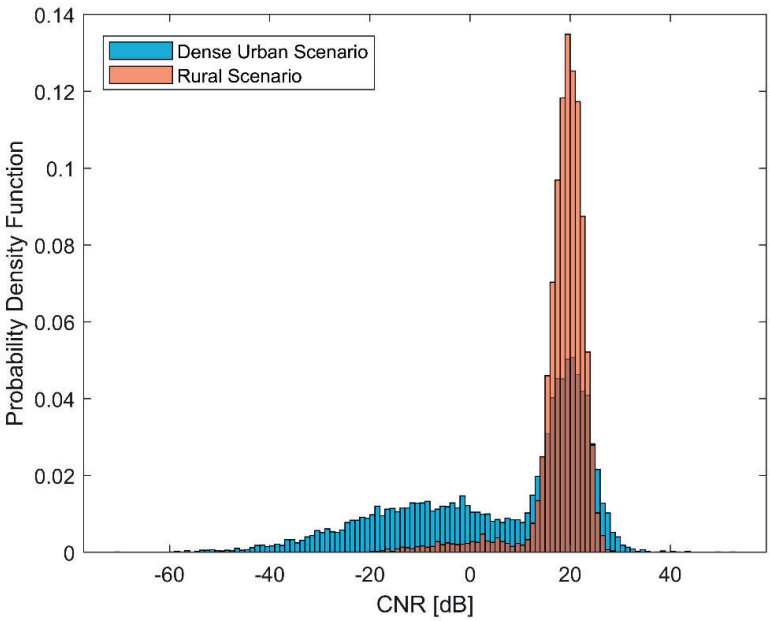

Fig. 23: The probability density function for the received signal CNR in rural and dense urban scenarios

4.4 Impact of Satellite Position Uncertainty

In the previous simulations, it was assumed that the exact satellite positions are known to the location server, but in reality, this is difficult to achieve. Due to the movement of the satellites, the satellite positions used by the location server are not precise. In these simulations, the uncertainty in the positions is a random variable with zero mean and standard deviation equals to 2 m, 5 m or 10 m. This uncertainty causes degradation in the positioning accuracy, as shown in Fig. 24. For 80% of the UEs, the positioning error is less than 2.8 m in the case of precisely known satellite positions, whereas it is less than 3.7 m in case of uncertain satellite positions with the standard deviation of 2 m, less than 6.8 m in case of uncertain satellite positions with the standard deviation of 5 m, and less than 13 m in case of uncertain satellite positions with the standard deviation of 10 m. This shows that, as the uncertainty in the satellite positions increases, the positioning error increases as well. Therefore, having accurate satellite positions (for example, to within 2 m) is essential for achieving good positioning estimation.

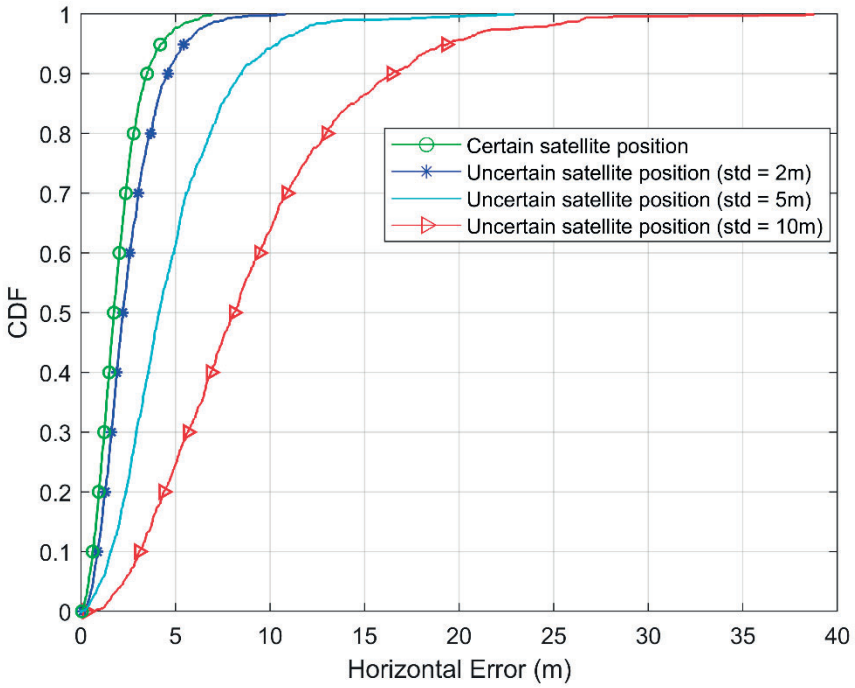

Fig. 24: Horizontal positioning accuracy for satellite position accuracy

CHAPTER 5

Summary and Future Work

In this thesis work, UE positioning accuracy in NTNs is investigated for the DL-TDOA method with respective to PRS configurations, satellite parameters, channel models and accuracy of satellite positions. The study was performed using a MATLAB simulator, which was developed based on existing code used for the study of positioning in TNs. PRS that supports different configurations was implemented to enable positioning using DL-TDOA.

Initially, different channel bandwidths were tested. Increasing the bandwidth leads to an increase in the proportion of UEs that have a positioning accuracy less than 3 m by 14%. Then, two further simulations were conducted in order to analyse the reasons behind this improvement. Firstly, the system was examined for different sampling frequencies. The results show that an increase in the sampling frequency has the dominant influence on the performance. Secondly, the system is evaluated for different number of PRS symbols transmitted per slot. It is observed that this parameter does not have much effect on the accuracy due to the high CNR inherent to the NTN setup in this study.

Satellite parameters were investigated as well. Firstly, the effect of the number of satellites for the estimation the UE location was examined. The results show that using 9 satellites outperforms the use of only 5 satellites by 14%, in terms of more UEs achieving the same positioning accuracy (of within 5 m). Secondly, the impact of the satellite altitude on the positioning accuracy was tested. The results show that the positioning accuracy in the case of using 600 km satellite altitude is better than in the case of using 1200 km satellite altitude, despite having similar CNR range in both cases. This is due to the increase in the error range by the increase of the satellite altitude.

Two channel deployment scenarios were also implemented and tested in the simulator, which are rural scenario and dense urban scenario. The simulation results show that the rural scenario has higher positioning accuracy than the

dense urban scenario. This is primarily because the rural scenario has higher probability of LOS than the dense urban scenario for all elevation angles.

To show the importance of synchronization, a simulation is performed using non-precise satellite positions. The satellite position is modelled with random uncertainty with zero mean and a predefined standard deviation. The results show that the performance degrades as the uncertainty in the satellite position increases.

For future work, positioning accuracy can be further improved by investigating the possibility of combining different cellular positioning techniques in NTN. Moreover, the possibility of implementing carrier phase-based positioning in NTN will be interesting to be investigated, as it can improve the accuracy down to the millimetre range [21]. However, this effort may be challenging because of the complexity of finding a feasible ambiguity integer. Furthermore, the impact of time synchronization and significant timing delays of the received signal from different satellites on accuracy performance can be evaluated. In addition, multiband positioning for different satellite systems (LEO, MEO and GEO) can be investigated to improve positioning accuracy. The work can be extended as well to include Machine-to-Machine (M2M) and Internet-of-Things (IoT) devices instead of only 5G NR handheld devices.

Bibliography

[1] F. Rinaldi *et al*., "Non-Terrestrial Networks in 5G & Beyond: A Survey," in *IEEE Access*, vol. 8, pp. 165178-165200, 2020.

[2] 3GPP TS 38.821, *Solutions for NR to support non-terrestrial networks (NTN) (Release 16).* Technical Specification Group Radio Access Network; 38.821. Version 16.0.0. 3rd Generation Partnership Project (3GPP), Dec. 2019.

[3] X. Lin, S. Rommer, S. Euler, E. A. Yavuz and R. S. Karlsson, "5G from Space: An Overview of 3GPP Non-Terrestrial Networks," arXiv:2103.09156, 2021.

[4] J. A. del Peral-Rosado, R. Raulefs, J. A. Lopez-Salcedo and G. Seco-Granados, "Survey of Cellular Mobile Radio Localization Methods: From 1G to 5G," in *IEEE Communications Surveys Tutorials*, vol. 20 no. 2, pp. 1124-1148, 2018.

[5] 3GPP TS 38.305. *NG Radio Access Network (NG-RAN); Stage 2 functional specification of User Equipment (UE) positioning in NG-RAN (Release 16)*. Technical Specification Group Radio Access Network; 38.305. Version 16.0.0. 3rd Generation Partnership Project (3GPP), Mar. 2020.

[6] D. Ugur Sanli, "Introductory Chapter: The Philosophy Behind the Accuracy Assessment of GNSS Methods," in *Accuracy of GNSS Methods*, IntechOpen, 2019.

[7] R. Wu, W. Wang, D. Lu, L. Wang and Q. Jia, "Principles of Satellite Navigation System," in *Navigation: Science and Technology*, Springer Singapore, 2017, pp. 1–29.

[8] J. L. Awange, "The Global Positioning System," in *Environmental Science and Engineering*, Springer Berlin Heidelberg, 2012, pp. 23–39.

[9] M. Tamazin, M. Karaim, and A. Noureldin, "GNSSs, Signals, and Receivers," in *Multifunctional Operation and Application of GPS*, InTech, 2018.

[10] L. Pan et al., "Satellite availability and point positioning accuracy evaluation on a global scale for integration of GPS, GLONASS, BeiDou and Galileo," in *Advances in Space Research*, vol. 63, no. 9, pp. 2696–2710, May 2019.

[11] D. Doberstein, *Fundamentals of GPS Receivers*, New York: Springer, 2012.

[12] Z. Z. M. Kassas, J. Khalife, K. Shamaei and J. Morales, "I Hear, Therefore I Know Where I Am: Compensating for GNSS Limitations with Cellular Signals," in *IEEE Signal Processing Magazine*, vol. 34, no. 5, pp. 111-124, Sept. 2017.

[13] Z. (Zak) M. Kassas, "Navigation with Cellular Signals of Opportunity," in *Position, Navigation, and Timing Technologies in the 21st Century*. Wiley, pp. 1171–1223, Dec. 15, 2020.

[14] R. Keating, M. Saily, J. Hulkkonen and J. Karjalainen. "Overview of Positioning in 5G New Radio," in *2019 16th International Symposium on Wireless Communication Systems (ISWCS)*. 2019, pp. 320–324.

[15] S. Fischer, "OTDOA positioning in 3GPP LTE," Tech. Rep., Qualcomm Technologies Inc., 2014.

[16] S. Hu, A. Berg, X. Li and F. Rusek, "Improving the Performance of OTDOA Based Positioning in NB-IoT Systems," in *2017 IEEE Global Communications Conference (GLOBECOM 2017)*, Dec. 2017.

[17] 3GPP TS 38.211. *Physical channels and modulation (Release 16)*. Technical Specification Group Radio Access Network; 38.211. Version 16.0.0. 3rd Generation Partnership Project (3GPP), Dec. 2019.

[18] A. U. Chaudhry and H. Yanikomeroglu, "Laser Inter-Satellite Links in a Starlink Constellation," arXiv:2103.00056, 2021.

[19] 3GPP TS 38.811. *Study on New Radio (NR) to support non-terrestrial networks (Release 15)*. Technical Specification Group Radio Access Network; 38.811. Version 15.2.0. 3rd Generation Partnership Project (3GPP), Sep. 2019.

[20] 3GPP TS 38.900. *Study on channel model for frequency spectrum above 6 GHz (Release 14)*. Technical Specification Group Radio Access Network; 38.900. Version 14.3.1. 3rd Generation Partnership Project (3GPP), Aug. 2017.

[21] P. Henkel and C. Zhu, "Carrier Phase Integer Ambiguity Resolution with Inequality Constraints for GPS and Galileo," in *2011 IEEE Statistical Signal Processing Workshop (SSP)*, Jun. 2011.

Printed by Tryckeriet i E-huset, Lund 2021

LUND
UNIVERSITY

Series of Master's theses
Department of Electrical and Information Technology
LU/LTH-EIT 2021-838
http://www.eit.lth.se